Protein J (2011) 30:281–289
DOI 10.1007/s10930-011-9330-4

Expression and Purification of a Natural N-Terminal Pre-ligand Assembly Domain of Tumor Necrosis Factor Receptor 1 (TNFR1 PLAD) and Preliminary Activity Determination

Jin Cao · Fang Meng · Xiangdong Gao · Hongxia Dong · Wenbing Yao

Published online: 17 May 2011

Abstract A domain at the NH_2 terminal (N-terminal) of tumor necrosis factor receptor (TNFR) termed the pre-ligand binding assembly domain (PLAD). The finding that PLAD can mediate a selective TNFR assembly in previously researches provides a novel target to the prevention of TNFR signaling in immune-mediated inflammatory diseases (IMID). In this study, a natural N-terminal TNFR1 PLAD was obtained for the first time through the methods of GST-tag fusion protein expression and enterokinase cleavage. After purification with a Q Sepharose Fast Flow column, a natural N-terminal TNFR1 PLAD which purity was up to 95%, was obtained and was identified using Nano LC-ECI-MS/MS. Secondary structure analysis of PLAD was carried out using circular dichroism spectra (CD). After that, the TNFR1 PLAD in vitro anti-TNFα activity and the specific TNFR1 affinity were determined. The results proved that the natural N-terminal TNFR1 PLAD can selectively inhibit TNFα bioactivity mainly through TNFR1. It infers an effective and safe strategy for treating variety of IMID with a low risk of side effects in future.

Keywords Tumor necrosis factor receptor (TNFR) · Pre-ligand binding assembly domain (PLAD) · GST fusion protein · L929 cells

Abbreviations

TNFR	Tumor necrosis factor receptor
PLAD	Pre-ligand binding assembly domain
IMID	Immune-mediated inflammatory diseases
GST	Glutathione S-transferase
IPTG	Lactose analog isopropyl β-D-thiogalactoside
PVDF	Polyvinylidene difluoride membrane
MTT	(4,4-Dimethylthiazol-2-yl) 2,5-diphenyl tetrazolium bromide
OPD	o-Phenylenediamine dihydrochloride
LB	Luria-Bertani
ELISA	Enzyme-linked immunosorbent assay
DAB	Diaminobenzidine
TFA	Trifluoroacetic acid
CD	Circular dichroism spectra

J. Cao · F. Meng · X. Gao · H. Dong · W. Yao (✉)
School of Life Science and Technology, China Pharmaceutical University, Nanjing 210009, China
e-mail: wbyao@cpu.edu.cn

1 Introduction

Tumor necrosis factor α (TNFα) is a pleiotropic inflammatory cytokine which was first isolated by Carswell et al. in 1975. It has been proved that TNFα plays a central role in host defense and inflammation. It is believed that TNFα is involved in the development and exacerbation of the pathology of a variety of human diseases including rheumatoid arthritis, ankylosing spondylitis, inflammatory bowel disease, septic shock, multiple sclerosis, hepatitis and Alzheimer's disease, etc. [2, 6, 16, 22, 28].

TNFα mediates its biological effects by binding to two TNFα receptors, TNFR1 (also known as p55) and TNFR2 (also known as p75) [19]. Generally speaking, most of the TNFα activities, including inflammatory responses, are triggered by TNFR1, whereas TNFR2 plays an important role in regulating the immune response [3, 4, 21]. Because TNFα signaling has been implicated in the pathogenesis of wide variety of human diseases, especially inflammatory responses, TNFα has emerged as a major therapeutic target

in these disease [1, 10]. Recent years, anti-TNFα antibodies such as Infliximab (Humira®) and soluble TNFRs such as Etanercept (Enbrel®) have been used to treat various inflammatory diseases [15, 17]. Although these treatments in the clinic have yielded promising results, they can cause serious side effects, such as bacterial and virus infection, lymphoma development, lupus inflammatory disease [5, 20, 23, 24], as well as an increased risk of active tuberculosis [18]. The reason for these adverse effects is that the therapies with anti-TNFα antibody or soluble decoy receptor affect the TNFR2 mediated activities of TNF α, which are essential for immune function [27]. So the TNFα-dependent host defense functions are also inhibited. To overcome these problems, a new agent that selectively inhibits TNFα bioactivity through TNFR1 is highly desirable [26].

PLAD (pre-ligand binding assembly domain) is a conserved domain in the extracellular region of TNFR family, which contains three disulphide bridges. The function of TNFR PLAD was unknown until 2000. Reported by Francis Ka-Ming Chan, PLAD is physically distinct from the domain that forms the major contacts with ligand, but is necessary and sufficient for the assembly of TNFR complexes that bind TNF and mediate signaling [8]. PLAD can mediate a TNFR-trimer assembly with or without the ligand. So an efficient ligand-receptor binding relies on PLAD. Furthermore, the assembly of pre-ligand receptor complexes orchestrated by individual PLADs is receptor specific, that is to say, TNFR1 PLAD do not cross-bind the PLAD from TNFR2. These findings provide a novel target to the prevention of TNFR signaling in diseases such as rheumatoid arthritis. The PLAD can be an attractive alternative to design novel therapeutics against TNFR function [7, 9, 14]: TNFR1 PLAD is TNFR1 specific, so adverse effects mediated by TNFR2 can be avoided.

Guo-Min Deng et al. tested the GST-PLAD fusion protein as a therapeutic molecule in several mouse models of arthritis in 2005 [13] and in lupus MRL/lpr mice in 2009 [12]. The in vitro an in vivo data demonstrated that TNFR1 PLAD can potently inhibit TNFα and consequently ameliorate experimental inflammatory arthritis. Equally, TNFR1 PLAD significantly inhibited skin injury but TNFR2 PLAD failed to do so in MRL/lpr mice. However, the molecule they studied on was a TNFR1 PLAD fused with a GST-tag. They obtained GST-PLAD fusion protein by inserting fragment of PLAD into the multiple cloning site of the pGEX-4T1 vector, followed by expression in *E.coli* and purification of it. After that, they research the TNFR1 PLAD activities in vitro and in vivo without cleave the GST tag. Although they tested GST alone as a control group in activity studies, it is hardly being considered as a direct evidence of the effects of TNFR1 PLAD. The molecular weight of GST is about 32 kDa while PLAD is about 6 kDa, so the activity of PLAD might be affected by GST tag. In fact, Deng pointed out himself that the GST portion of the molecule should be removed from TNFR1 PLAD protein before using it as a treatment in humans [11].

To investigate the TNFR1 PLAD bioactivity better, a natural N-terminal TNFR1 PLAD was obtained through the methods of GST-tag fusion protein expression and enterokinase cleavage in our research. A pGEX-KG/GST-PLAD vector containing an enterokinase cleavage site was constructed by PCR and transformed into *E.coli* BL21 (DE3). The fusion protein was purified with a GSH-Agarose affinity column and the TNFR1 PLAD was purified from the enterokinase digest mixture with a Q Sepharose Fast Flow column. The TNFR1 PLAD in vitro anti-TNFα activity was determined by a TNFα-dependent L929 cells killing activity assay and the specific TNFR1 affinity was elementarily proved by a direct ELISA. The results proved for the first time that the TNFR1 PLAD without GST tag can selectively inhibit TNFα bioactivity mainly through TNFR1. It is inferred that a purified natural N-terminal TNFR1 PLAD can be a new agent that selectively inhibit TNFα bioactivity through TNFR1 blocking. It offers an effective and safe strategy for treating variety of IMID with a low risk of side effects.

In following context, PLAD is TNFR1 PLAD for short unless otherwise stated.

2 Materials and Methods

2.1 Materials

Expression vector pGEX-KG and Q Sepharose Fast Flow column were from GE Healthcare (Chalfont, UK). Restriction endonucleases BamHI and HindIII were from TaKaRa (Dalian, China). GSH-Agarose affinity column was purchased from Yihong (Shanghai, China). Enterokinase and mouse anti-GST antibody were from Sinobio (Shanghai, China). IPTG, PVDF membrane, MTT and OPD were from Sigma (St. Louis, MO). L929 cell was from Keygen (Nanjing, China). Actinomycin D, reduced glutathione and recombinant human TNFα (rhTNFα) were from Sangon (Shanghai, China). Horseradish-peroxidase conjugated goat anti mouse second IgG and DAB Horseradish Peroxidase Color Development Kit were purchased from Beyotime (Haimen, China). TNFR1 and TNFR2 are from Prospec (Rotherham, UK). All other regents were of the highest purity available.

2.2 Construction of Plasmid pGEX-KG/GST-PLAD

According to the reference, the full length of the TNFR1 PLAD protein sequence is LVPHLGDREK RDSVCPQGKY IHPQNNSICC TKCHKGTYLY NDCPGPGQDT DCR.

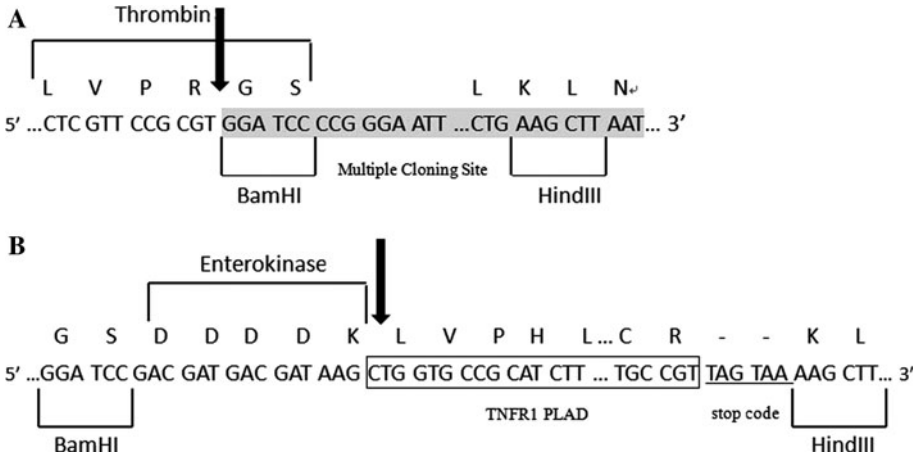

Fig. 1 Inserting enterokinase cleavage site into pGEX-KG plasmid by PCR to form the pGEX-KG/E-PLAD. **a** pGEX-KG plasmid with a thrombin cleavage site. **b** pGEX-KG/E-PLAD plasmid can express GST-PLAD fusion protein with an enterokinase cleavage site. After a site-specific cleavage, a natural N-terminal of PLAD can be obtained

DNA fragment encoding PLAD, as well as the stop codon were synthesized according to Escherichia coli codon usage preference by Genescript's gene synthesis services. A pair of primers was designed as below (the letter with underline was restriction endonucleases sites BamHI and HindIII) to insert the PLAD fragment into the pGEX-KG expression vector, which can sever a GST tag in C-terminal of the protein. A gene sequence of enterokinase (bold) was designed between the BamHI site and PLAD sequence to insert an enterokinase cleavage site in pGEX-KG vector instead of original thrombin cleavage site in pGEX-KG (Fig. 1). In this way, the expression product GST-PLAD can be cleaved by enterokinase to provide a natural N-terminal of TNFR1 PLAD.

5′ GGATCC**GACGATGACGATAAG**CTGGTGCCG CATCTTG 3′

5′ AAGCTTTTACTAACGGCAATCGGTA 3′

PLAD fragment with enterokinase site and two restriction endonucleases was amplified by PCR. The PLAD fragment was digested by restriction endonucleases BamHI and HindIII and then inserted into the pGEX-KG to form the pGEX-KG/GST-PLAD. The recombinant plasmid of pGEX-KG/GST-PLAD was used to transform E.coli BL21 (DE3) and resultant colonies were screened by ampicillin and PCR.

2.3 Expression and Purification of GST-PLAD

The engineer E. coli BL21 (DE3) was fermented in LB medium containing ampicillin in flask at 37 °C and induced by 0.3 mM IPTG at OD600 of 1.0 for 7 h. The cultured cells were collected by centrifugation, followed by being mixed and suspended with balance buffer (140 mM NaCl, 10 mM Na_2HPO_4, 1.8 mM K_2HPO_4, pH 7.5). The cells were broken by ultrasonic treatment. The soluble protein in the supernatant was separated with the precipitate after centrifugation.

The pH of the supernatant was adjusted to 7.5 with 1 M NaOH. After that, the sample was applied to a GSH-Agarose column pre-equilibrated with balance buffer. The fraction was eluted and collected with 5–10 column volumes of elution buffer (50 mM Tris–HCl, 33 mM glutathione, pH 7.5) after the column was washed with 5–10 column volumes of balance buffer. Maintain flow rates of 1 ml/min. The fractions were analysis by sodium dodecyl sulfate–polyacrylamide gel electrophoresis (SDS–PAGE). Protein bands were stained with Coomassie brilliant blue G250.

2.4 Cleavage of GST-PLAD by Enterokinase and Purification of PLAD

The concentration of GST-PLAD solution was determined by UV adsorption using a calculated molar extinction coefficient of 47955 $M^{-1}cm^{-1}$ at 280 nm (analysis by ExPASy Proteomics Server). After knowing the amount of GST-PLAD, add 0.5 mμl enterokinase solution for each mg of GST-PLAD fusion protein. For digestion is complete, incubate the digest mixture at room temperature for 8 h. Then load the digest mixture onto the Q Sepharose Fast Flow column pre-equilibrated with 50 mM Tris–HCl (pH 7.5), keeping a flow rate of 2 ml/min. Analysis by ExPASy proteomics sever on line, the PI of PLAD is 7.8. In buffer pH 7.5 PLAD carries a positive charge, so it cannot be adsorbed by Q Sepharose Fast Flow and flowed through. The OD280 of the effluent was monitored. The fractions containing proteins were collected and analysis by Tricine-SDS–PAGE. GST tag and other proteins, including enterokinase, were adsorbed on the column and can be eluted by elution buffer (50 mM Tris–HCl, 1 M NaCl, pH 7.5).

2.5 Western Blotting

For western blotting the proteins were electroblotted onto a PVDF membrane, 1 mA/cm^2 for 1.5 h. Proteins were reacted with a primary antibody (mouse anti-GST antibody) at a dilution of 1:500 and a secondary antibody (horseradish-peroxidase conjugated goat anti mouse second

IgG) at a dilution of 1:5000. The target proteins on the membrane were detected by a DAB Horseradish Peroxidase Color Development Kit.

2.6 RP-HPLC Purity Analysis

The purify of PLAD was determined by analytical RP-HPLC with a reverse-phase column (5 μm, 250 × 4.6 mm I.D., YMC-Pack C18). The following conditions were utilized: a linear gradient of mobile phase 5–95% B in 35 min (mobile phase A: water with 0.1% TFA, mobile phase B: acetonitrile with 0.1% TFA) at a flow rate of 1 ml/min, and ultraviolet (UV) detection at 280 nm.

2.7 Nano LC–ESI–MS/MS

The protein identification work was carried out at ProtTech, Inc. (Norristown, PA) by using the Nano LC–ESI–MS/MS peptide sequencing technology. In brief, digested in-gel with sequencing grade modified trypsin and the dissolved peptide samples was then injected into a high pressure liquid chromatography (HPLC) system with a 75 μm inner diameter reverse phase C18 column. The HPLC system was on-line coupled with an ion trap mass spectrometer in a way a sample eluted from HPLC column was ionized by an electrospray ionization (ESI) process and enter into the mass spectrometry.

The mass spectrometric data acquired were used to search the most recent non-redundant protein database with ProtTech's proprietary software suite.

2.8 Circular Dichroism Spectra (CD)

Secondary structure analysis of the PLAD was carried out using circular dichroism spectra (CD). CD were recorded at room temperature on a Jasco J-810 specropolarimeter equipped. Samples containing 0.3 mg/ml of PLAD in double distilled water was used for far-UV measurements. Spectra were recorded from 190 to 250 nm with 1 nm resolution at 100 nm/min. The cuvette used for far-UV spectral recording has path length of 0.1 cm. Data was analysised with Jasco Secondary Structure Estimation.

2.9 Neutralization of TNFα-Induced Cytotoxicity in L929 Cells

Human recombinant TNFα causes cell cytotoxicity to murine L929 cells after an incubation period of 18–24 h. The PLAD in vitro activity assay was carried out as follow. L929 cells were digested by trypsin and suspended in the 10% bovine serum DMEM at a density of 10^5 cells/ml, and add 100 μl/well to 96-well flat-bottom culture plates. The plates were then incubated overnight at 37 °C in 5% CO2. 18–24 h later, 50 μl different concentrations of PLAD, GST-PLAD or etranscept (positive control group), as well as 50 μl actinomycin D (2 μg/mL final concentration) were added to each well and incubated for another 2 h. After that, 50 μl rhTNFα (2 ng/ml final concentration) was added to each well, followed by 18-h incubation. 20 μl of 5 mg/ml MTT in PBS was added. The plates were then incubated for 4 h at 37 °C. The supernatant was removed from each well and 150 μl DMSO was added. After shaking the plates for 5 min, the optical density at 490 nm was measured in a microplate reader. The values of blank control group were A_0, while the values of sample groups were A_S, the growth ratio $G = (A_S - A_0)/A_0$. Uncertainty of the growth ratio was calculated using this uncertainty transfer equations: $\frac{\Delta G}{G} = \sqrt{\left(\frac{\Delta A_s}{A_s}^2\right) + \left(\frac{\Delta A_0}{A_0}\right)^2}$.

In this test 6 replicates were used in each concentration group.

2.10 Affinity Assay Test by ELISA

To determine the affinity of PLAD for TNFR1 and TNFR2, a direct enzyme-linked immunosorbent assay (ELISA) was taken. The steps of this method were as follows. First, microtiter plates were coated with 100 ng/well recombinant human TNFR1 or TNFR2 at 37 °C for 2 h. After being rinsed 3 times with PBS-Tween 20 (PBST), the plates were blocked with 10% bovine serum at 37 °C for 1 h. Plates were rinsed for another 3 times before 100 μl gradient diluted GST-PLAD solution were added to each well. After plates were incubated at 37 °C for 1 h and rinsed thrice, mouse anti-GST antibody (1:500 diluted with PBS containing 4% FCS) was added for 1 h at 37 °C. Than the plates were washed and added with horseradish-peroxidase conjugated goat anti mouse second IgG at a dilution of 1:10000. After a 37 °C incubation for 1 h, the plates were washed and the bound peroxidase activity was measured by adding 100 μl/well OPD solution (phosphate-citrate buffer, pH 5.0, 0.003% H2O2, 40 μg/ml OPD) for 15 min at 37 °C. The reaction was stopped by 2 M H2SO4. Absorbance (492 nm) of wells was measured in a microplate reader. The data was analysis by SigmaPlot 10.0 software and fitting curves was formed. Furthermore, EC50 of both TNFR1 and TNFR2 were obtained.

3 Results and Discussion

3.1 Construction of Plasmid pGEX-KG/GST-PLAD

PLAD is a 6 kDa peptide with three pairs of disulfide bonds, so it is not fit for direct expression. On one hand, our

lab has had a try on the direction of expressing PLAD in a bacterial expression system without any partners and has failed. Furthermore, if the protein is expressed as inclusion body, renaturation and refolding can increase the frequency of incorrect disulfide bands. On the other hand, "N–N–S" in PLAD amino acid sequence is a potential N-glycosylation site. If PLAD express in a *Pichia pastoris* expression system, a sugar chain may be added to the protein. Because N-glycosylation of protein might lead to some changes in molecular structure and activity, *Pichia pastoris* is also not a suitable expression system for PLAD.

In the view of the above-mentioned causes, co-expressing with a solubility enhancing tag is a good strategy to enhance the soluble expression and the correct pairing of disulfide bonds. pGEX-KG vector contains a *ptac* transcriptional promoter to express GST fusion protein. But the site specific protease sequence is for thrombin cleavage, which cleavage site is LVPR/GS. In order to obtain a natural N-terminal PLAD, an enterokinase cleavage site was inserted in pGEX-KG vector instead of thrombin cleavage site by PCR (Fig. 1).

The reconstructed plasmid pGEX-KG/GST-PLAD was identified by enzyme digestion and DNA sequencing.

3.2 Expression, Purification and Characterization of GST-PLAD

The expression vector pGEX-KG/GST-PLAD uses a pBR322 origin. The presence of the *lacIq* gene on the pGEX-KG plasmid assures that the lac repressor not be transcribed until induced by IPTG. Fig. 2a shows that after induction, the engineering bacteria BL21 (DE3) can express a major band with a molecular weight between 31 and 43 kDa. It shows a good agreement with the theoretical value of GST-PLAD (32 kDa). The GST helps to provide a good yield of non-degraded fusion protein in the soluble fraction. Besides, the GST serves as a tag for purification and determination of the fusion protein. As shown in Fig. 2b, recombinant fusion protein GST-PLAD can be adsorbed by GSH-agarose column and eluted by 33 mM reduced glutathione in 50 mM Tris-HCl, pH 7.5. The elution was collected and the concentration was determined by UV adsorption using a calculated molar extinction coefficient of 47955 M^{-1} cm^{-1} at 280. The other proteins flowed through the column, and the effluent was collected, too.

Western blotting was taken to determine if this recombinant protein is a fusion protein containing a GST tag. As shown in Fig. 3, in high concentration, a major band about 31 kDa and a slim band about 66.2 kDa can be observed in SDS–PAGE. According to the western blotting result, both of these two proteins can reacted with GST antibody. It demonstrated that the major band is GST-PLAD fusion protein, and the other is GST-PLAD dimer because of the dimerization from GST.

3.3 Enterokinase Cleavage and Purification of PLAD

The fusion protein GST-PLAD was cleaved with enterokinase at the exactly site of the first N-terminal amino acid of PLAD. According to Fig. 4 the Tricine-SDS–PAGE result, after incubation with the enterokinase enzyme at

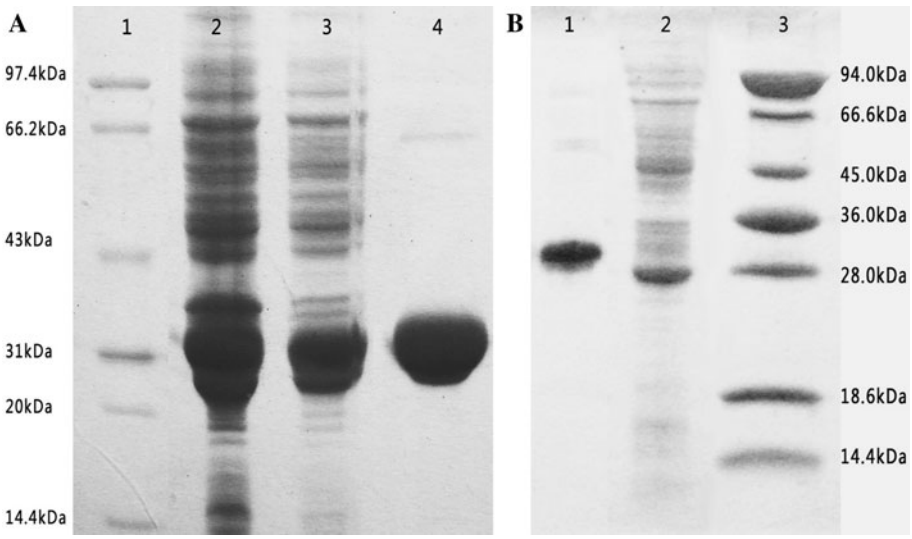

Fig. 2 Preparation of GST-PLAD fusion protein by GSH-Agarose affinity column. Proteins were detected on 12% SDS–PAGE and stained with Coomassie brilliant blue. **a,** Expression and purification of GST-PLAD. *Lane 1*: protein molecular weight marker; *Lane 2*: total proteins after induction; *Lane 3*: supernatant after ultrasonic; *Lane 4*: purified GST-PLAD fusion protein. **b,** Effect of GSH-Agarose column for purification of GST-PLAD. *Lane 1*: GST-PLAD fusion protein eluted using 33 mM reduced glutathione; *Lane 2*: other proteins in effluent; *Lane 3*: protein molecular weight marker

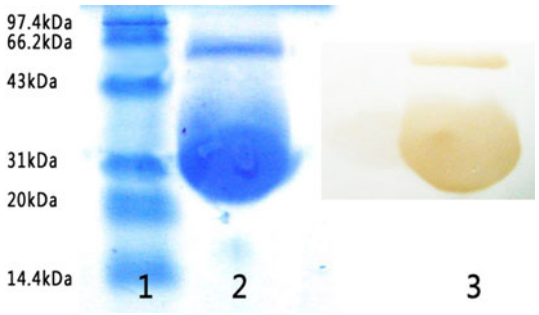

Fig. 3 Western blotting to detected the GST-tag in the fusion protein. *Lane 1*: protein molecular weight marker; *Lane 2*: GST-PLAD detected on 12% SDS–PAGE and stained with Coomassie brilliant blue; *Lane 3*: fusion protein transferred to PVDF membrane and reacted with GST antibody

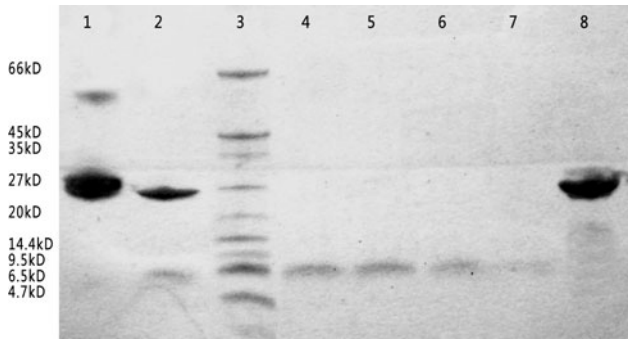

Fig. 4 Enterokinase cleavage and purification of PLAD by Q Sepharose Flas Flow column. The proteins samples were analysis on 16% Tricine-SDS–PAGE and stained with Coomassie brilliant *blue*. *Lane 1*: GST-PLAD before cleavage; *Lane 2*: GST-PLAD after cleavage; *Lane 3*: low range protein molecular weight marker; *Lane 4–7*: after Q Sepharose Fast Flow column purification: PLAD in the effluent; *Lane 8*: other proteins eluted with 1 M NaCl

room temperature, a strong decrease of fusion protein band was observed, showing that cleavage of GST-PLAD was possible. Site-specific cleavage without any mistake has high activity to digest GST-PLAD completely.

In addition, a band near the 6.5 kDa molecular weight marker was obtained, that is similar to the theoretic molecular weight of PLAD. After purification by Q Shepharose Fast Flow column, the effluent of the column was collected as while as the 1 M NaCl elution. Basic protein PLAD in digest mixture carried a positive charge and flowed through Q Sepharose Fast Flow when pH of the column buffer is 7.5. The other proteins, including GST, reduced glutathione and enterokinase in the digest mixture were adsorbed on the column for they are all acidic proteins. Figure 4 also suggests that the PLAD was purified from the digest mixture, and the other proteins were in elution. The major part of elution was GST.

Other strategies, including GSH-Agarose column and cation exchange column (SP Sepharose Fast Flow) had been used for PLAD purification from digest mixture in our lab. Unfortunately, the target protein getting from these columns was mixed with GST protein. The reason may be the affinity of GSH-Agarose column or the adsorbility of SP Sepharose Fast Flow column are not strong enough to get a satisfactory separation result. On-column cleavage had also been tried, but the cleavage effect and separation results after cleavage were unsatisfactory, and the yield rate of PLAD is low. On the other hand, the balance buffer is 50 mM Tris-HC (pH 7.5) when Q Sepharose Fast Flow column is used, as same as the enterokinase cleavage buffer and GST-Agarose column elution buffer. Therefore, several dialysis steps can be skipped to reduce work amount and to save time.

3.4 RP-HPLC Purity Analysis

To determine the purity of PLAD, analytical RP-HPLAC was employed. The Fig. 5 result suggested that the purity of PLAD was up to 95%. Purified PLAD was used in the cell activity detection and affinity test.

3.5 Nano LC–ESI–MS/MS

A customized database search was carried to identify this protein. With the customized database search, several overlapping N-terminal peptides were identified as Fig. 6. It is clear that these peptides sequence are exactly the same as the N-terminal of PLAD. The result confirms the identification of the PLAD we obtained as a natural N-terminal PLAD.

However, in this LC–ESI–MS/MS analysis only one N-terminal peptide is identified. The poor peptide coverage is mainly due to the poor recovery of Cys-containing peptides from in-gel trypsin digestion. The alkylation reaction of proteins in a gel band is not effective. If Cys residues are not alkylated, they are normally not recovered. Generally speaking, Cys-containing peptides normally account for 0–20% of total peptides in a trypsin digestion

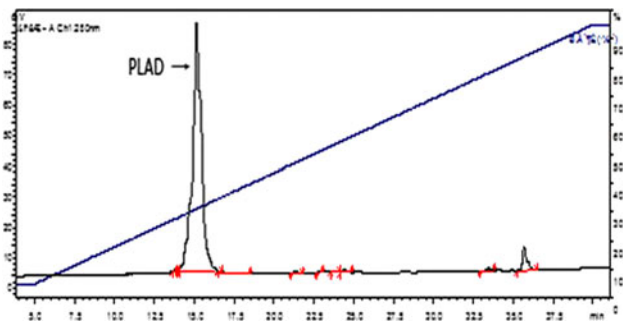

Fig. 5 RP-HPLC purity analysis. To determine the purity of PLAD, analytical RP-HPLC was employed. The result suggested that the purity of PLAD was up to 95%

A

Scan No.	Peptide Mass	Peptide Sequence
2615	1318.75	LVPHLGDREKR
2643	1162.65	LVPHLGDREK
2671	905.51	LVPHLGDR
2953	905.51	LVPHLGDR
3179	1162.65	LVPHLGDREK
3273	905.51	LVPHLGDR

B

1 LVPHLGDREK RDSVCPQGKY IHPQNNSICC TKCHKGTYLY NDCPGPGQDT
51 DCR

C

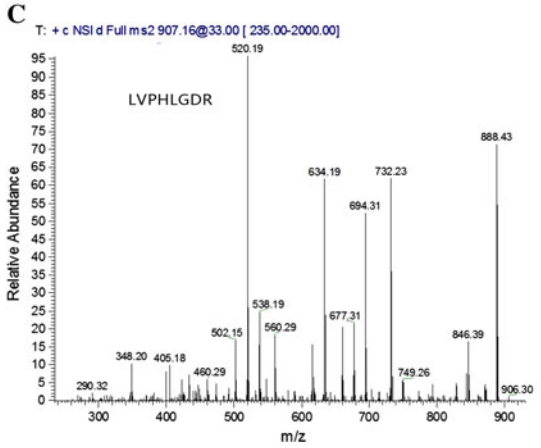

Fig. 6 Identification of PLAD. Purified PLAD was analysis by Nano LC–ESI–MS/MS. **a**, Report provided by ProtTech. *Peptide Mass*: The calculated molecular weight of each peptide based on its amino acid sequence. *Peptide Sequence*: The sequence of each peptide identified. **b**, Amino acid sequence of the PLAD. **c**, Nano LC–ES–MS/MS spectra of PLAD in-gel digestion

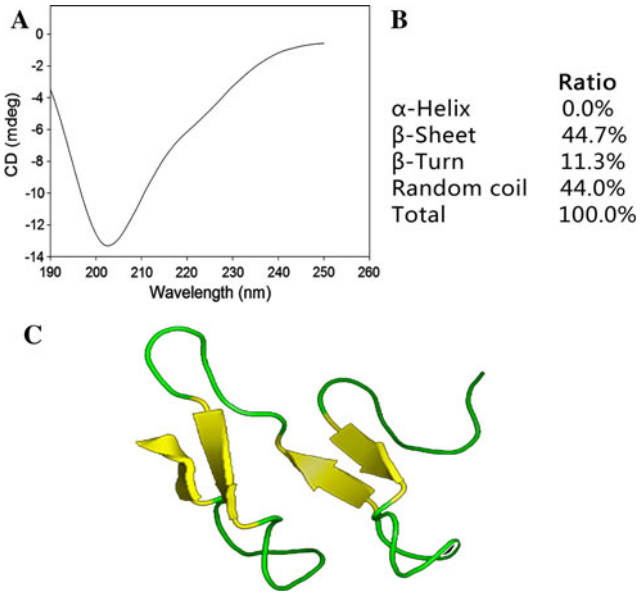

Fig. 7 Circular dichroism spectra (CD) for secondary structure. The secondary structure of PLAD was confirmed by CD spectral analysis. **a**, Far UV-CD spectrum of PLAD. **b**, Secondary structure analysis result. **c**, Predicted three dimensions structure performed by PyMOL. Both CD spectral analysis result and predicted three dimensions structure show that there is no α-helix in the PLAD content

in a typical protein, the missing of Cys-containing peptides is not a problem for protein identification. However, all peptides from trypsin digestion of PLAD are Cys-containing peptides, except the N-terminal peptide. So the N-terminal peptide is the only recovery one. But it is still clear that we obtained a natural N-terminal PLAD.

3.6 Circular Dichroism Spectra (CD)

The secondary structure of PLAD was confirmed by CD spectral analysis. The results show that PLAD had no α-helix content, and the ratio of *β*-sheet, *β*-turn and random coil were 44.7, 11.3 and 44.0% (Fig. 7a, b). The three dimensions structure predicted by ExPAsy sever on line revealed similar results (fig. 7c).

There are something else known about PLAD structure and function. In 2000, Francis Ka-Ming Chan et al. found out that two substitutions in PLAD can disturb TNFα binding and receptor function. Like a PLAD-deletion-TNFR1, $Lys^{19}Tyr^{20} \rightarrow Ala^{19}Ala^{20}$ (KY19/20AA) and $Lys^{32} \rightarrow Ala^{32}$ (K32A) mutations did not confer any protection against TNF-induced death in all experiments [8]. It can be inferred that Lys^{19}, Tyr^{20} and Lys^{32} (labeled in Fig. 8) could be the active sites of PLAD binding function. We proposed that the 3 pairs of disulfide bonds between Cys^{15}-Cys^{29}, Cys^{30}-Cys^{43} and Cys^{33}-Cys^{52} are important in maintaining the stable 3D structure of PLAD. They are also necessary to keep the correct position of Lys^{19}, Tyr^{20} and Lys^{32} to acquire the optimum spatial orientations and distances to be functionally effective.

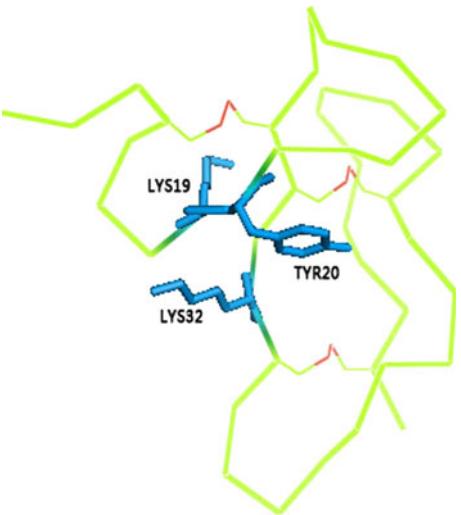

Fig. 8 Three dimensions structure of PLAD. The *figure* was prepared by using PyMOL

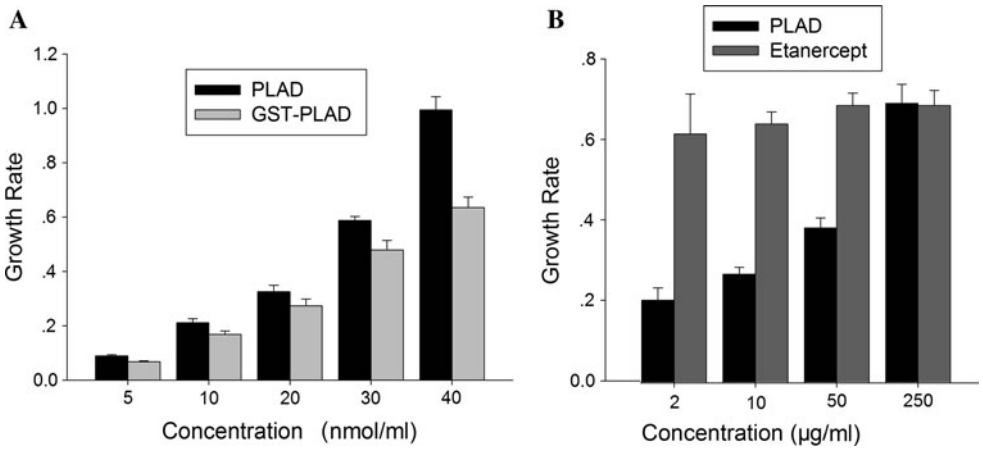

Fig. 9 The activity of the purified GST-PLAD and PLAD determined by TNFα-dependent L929 cells killing activity assay. **a**, Purified GST-PLAD or PLAD inhibited TNFα-induced cell death in a dose-dependent fashion. **b**, PLAD could significantly inhibit TNFα when its concentration rising to 250 μg/ml, it, being equally effective as etanercept

3.7 Neutralization of TNFa-Induced Cytotoxicity in L929 Cells

To determine the activity of the purified GST-PLAD and PLAD, we performed a TNFα-dependent L929 cells killing activity assay based on the method described by Kathleen et al. [25]. The L929 cells in exponential phase were first pretreated with GST-PLAD or PLAD to block the TNFR1 trimerization site so the TNFα cytotoxicity can be avoided. The protection was comparable to that conferred by etanercept. According to Fig. 9a, cell growth was decreased by TNFα induction, and purified GST-PLAD or PLAD inhibited TNFα-induced cell death in a dose-dependent fashion. The ability of the protection was increased after GST-tag was removed. It implied that GST-tag did not inhibit cell death. In a word, the result suggested purified GST-PLAD or PLAD can inhibit the cytotoxicity effect of TNFα on L929 cells. As shown in Fig. 9B, compared with etanercept, the activity of PLAD in low dose is less effective. But with PLAD concentration rising to 250 μg/ml, it could significantly inhibit TNFα, being equally effective as etanercept.

3.8 Affinity Assay Test by ELISA

The direct ELISA descripted above was used to determine the affinity of PLAD for TNFR1 and TNFR2. The absorbance at 492 nm was proportional to the GST-PLAD in a dose-dependent fashion. A scatter plot was drawn taking GST-PLAD concentration as abscissa axis (*X*) and absorbance as longitudinal axis (*Y*). SigmaPlot 10.0 software was used to analysis the data and to get the fitting curves and EC50 of both TNFR1 and TNF2. According to the results in Fig. 10, the EC50 of PLAD to TNFR1 is 0.0893, while the EC50 of PLAD to TNFR2 is 0.0165. It can be inferred that the affinity of PLAD for TNFR1 is higher than TNFR2, showing a fairly good agreement with the earlier conclusion from references.

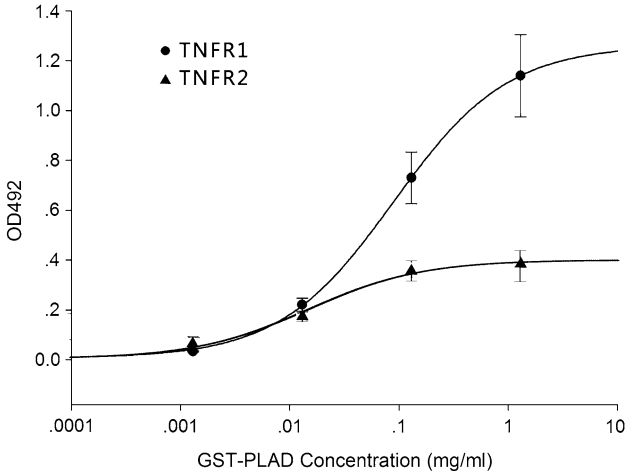

Fig. 10 The fitting curves for the PLAD affinity to both TNFR1 and TNFR2. Analysis by SigmaPlot 10.0, the EC50 of PLAD to TNFR1 is 0.0893, much higher than the TNFR2 EC50 0.0165. It suggested that the affinity of PLAD to TNFR1 is higher than it to TNFR2

The results of TNFα-dependent L929 cells killing activity assay and direct ELISA are in line with the previous works by Chan and Deng. It is proved for the first time that the purified PLAD can selectively inhibit TNFα bioactivity mainly through TNFR1. However, more tests should be taken in further researches to confirm these preliminary results, including in vivo anti-TNFα activity assay and other affinity and specificity experiments such as surface plasmon resonance (SPR) assay.

4 Conclusion

In this study, a natural N-terminal TNFR1 PLAD was obtained for the first time through the methods of GST-tag fusion protein expression and enterokinase cleavage and was identified using Nano LC-ECI-MS/MS and circular

dichroism spectra. The results from the in vitro anti-TNFα activity assay and the affinity test proved that untagged PLAD with the native N-terminal sequence can selectively inhibit TNFα bioactivity mainly through TNFR1. It is inferred that TNFR1 PLAD can be a new agent that selectively inhibit TNFα bioactivity through TNFR1 blocking. It offers an effective and safe strategy for treating variety of IMID with a low risk of side effects in future.

Acknowledgments This study was supported by grants from the Jiangsu Provincial Research Innovation Program for College Graduates (CX09B_290Z) and Qing Lan Project.

References

1. Adachi T, Toishi T, Takashima E, Hara H (2006) Biol Pharm Bull 10(29):2095–2098
2. Aderka D, Engelmann H, Maor Y, Brakebusch C, Wallach D (1992) J Exp Med 2(175):323–329
3. Aggarwal BB, Eessalu TE, Hass PE (1985) Nature 6047(318): 665–667
4. Bradley JR (2008) J Pathol 2(214):149–160
5. Brown SL, Greene MH, Gershon SK, Edwards ET, Braun MM (2002) Arthritis Rheum 12(46):3151–3158
6. Chadwick W, Magnus T, Martin B, Keselman A, Mattson MP, Maudsley S (2008) Trends Neurosci 10(31):504–511
7. Chan FK (2000) Ann Rheum Dis 59(Suppl 1):i50–i53
8. Chan FK, Chun HJ, Zheng L, Siegel RM, Bui KL, Lenardo MJ (2000) Science 5475(288):2351–2354
9. Chan KF, Siegel MR, Lenardo JM (2000) Immunity 4(13): 419–422
10. Chen G, Goeddel DV (2002) Science 5573(296):1634–1635
11. Deng GM (2007) BioDrugs 1(21):23–29
12. Deng GM, Liu L, Tsokos GC (2009) J Immunol 182 Meeting Abstract Suppl: 50.24
13. Deng GM, Zheng L, Chan FK, Lenardo M (2005) Nat Med 10(11):1066–1072
14. Deng GM, Lenardo M (2006) Drug Discov Today Dis Mech 2(3):163–168
15. Feldmann M (2002) Nat Rev Immunol 5(2):364–371
16. Feldmann M, Maini RN (2003) Nat Med 10(9):1245–1250
17. Goldbach-Mansky R, Lipsky PE (2003) Annu Rev Med 54:197–216
18. Gomez-Reino JJ, Carmona L, Valverde VR, Mola EM, Montero MD (2003) Arthritis Rheum 8(48):2122–2127
19. Jones DS, Silverman AP, Cochran JR (2008) Trends Biotechnol 9(26):498–505
20. Keane J, Gershon S, Wise RP, Mirabile-Levens E, Kasznica J, Schwieterman WD, Siegel JN, Braun MM (2001) N Engl J Med 15(345):1098–1104
21. MacEwan DJ (2002) Cell Signal 6(14):477–492
22. Muto Y, Nouri-Aria KT, Meager A, Alexander GJ, Eddleston AL, Williams R (1988) Lancet 8602(2):72–74
23. Nathan DM, Angus PW, Gibson PR (2006) J Gastroenterol Hepatol 9(21):1366–1371
24. Shakoor N, Michalska M, Harris CA, Block JA (2002) Lancet 9306(359):579–580
25. Sheehan KC, Pinckard JK, Arthur CD, Dehner LP, Goeddel DV, Schreiber RD (1995) J Exp Med 2(181):607–617
26. Shibata H, Yoshioka Y, Ohkawa A, Minowa K, Mukai Y, Abe Y, Taniai M, Nomura T, Kayamuro H, Nabeshi H, Sugita T, Imai S, Nagano K, Yoshikawa T, Fujita T, Nakagawa S, Yamamoto A, Ohta T, Hayakawa T, Mayumi T, Vandenabeele P, Aggarwal BB, Nakamura T, Yamagata Y, Tsunoda S, Kamada H, Tsutsumi Y (2008) J Biol Chem 2(283):998–1007
27. Shibata H, Yoshioka Y, Ohkawa A, Abe Y, Nomura T, Mukai Y, Nakagawa S, Taniai M, Ohta T, Mayumi T, Kamada H, Tsunoda S, Tsutsumi Y (2008) Cytokine 2(44):229–233
28. Shibata H, Yoshioka Y, Abe Y, Ohkawa A, Nomura T, Minowa K, Mukai Y, Nakagawa S, Taniai M, Ohta T, Kamada H, Tsunoda S, Tsutsumi Y (2009) Biomaterials 34(30):6638–6647